JOURNAL OF CATALYSIS **156**, 273–278 (1995)

Ab Initio SCF MO Study of the Chemisorption of Methane on Al and La Oxide Surfaces

María José Capitán,* José Antonio Odriozola,* Antonio Márquez,† and Javier Fernández Sanz†

**Department of Inorganic Chemistry, University of Sevilla, E-41012 Sevilla, Spain; and †Department of Physical Chemistry, Faculty of Chemistry, University of Sevilla, E-41012 Sevilla, Spain*

Received September 23, 1994; revised March 29, 1995; accepted June 20, 1995

A theoretical approach to the rate-determining step for methane activation on Al and La oxides has been performed by means of ab initio quantum mechanical calculations. In a first approach, transition states and products for the heterolytic chemisorption of CH_4 on $Al(OH)_3$ and $La(OH)_3$ molecules have been determined at the RHF-SCF level of theory. Transition-state structures correspond to a four-center interaction with an energy barrier of about 40 kcal/mol. This high activation barrier supports the heterolytic mechanism proposed for this reaction. The products are methyl–metal compounds, CH_3–Me (Me = Al, La), with the carbon atom negatively charged. Catalytic surfaces have been modeled by introducing the effects due to the lattice through both point charges and ab initio model potentials. The selectivity of these catalysts towards C2 is discussed on the grounds of the differences found for the relative stability of the methyl–metal intermediates.

INTRODUCTION

Activation of hydrocarbon C–H bonds is one of the most exciting topics in the field of heterogeneous catalysis. The possibility of converting the relatively abundant methane, the main component of natural gas, into higher carbon derivatives of synthetic interest (such as ethane and ethylene) has attracted considerable attention in the scientific community (1).

The global reaction for the catalyzed oxidation of methane can be written as

$$CH_4 + O_2 \underset{[cat]}{\longrightarrow\!\!\!\rightarrow\!\!\!\rightarrow} C_2H_6 + C_2H_4 + CO_x + H_2O,$$

and in this process the selectivity of the catalysts are usually defined in terms of ethane and ethylene yield (C2 products) while activity refers to the catalytic capacity whatever the reaction products are.

For the dehydrodimerization (2) of methane to yield ethane and ethylene, a wide variety of catalysts have been reported, among them alkali-doped alkaline earth metal oxides (3–5) and lanthanide oxides (pure and supported) (6) have shown high activity and selectivity. However, the selectivity of the process towards C2 products has been shown to be quite sensitive with respect to the nature and the pretreatment of catalysts. Hence, we have recently performed an experimental systematic study of this process using lanthanide oxides supported on γ-Al_2O_3 as catalysts (7). Pure γ-Al_2O_3 is slightly active and totally inefficient towards C2. For low loading of lanthanide-supported catalysts, higher activity and selectivity have been observed when the Ln_2O_3/γ-Al_2O_3 ratio is increased. The maximum of selectivity is found for a loading of about 5–10% and corresponds to surfaces in which the lanthanide ion is highly dispersed. For higher loading, while the oxidative activity increases, the selectivity towards C2 lowers, reaching a minimum for a ratio of 1. Effectively, mixed oxides such as $AlLaO_3$ and $AlSmO_3$ are highly effective as total oxidative catalysts. It is worth noting that the structure of these 1 : 1 mixed oxides can no longer be considered as doped γ-Al_2O_3 but are of the perovskite type. Further addition of lanthanide raises the selectivity, reaching a second maximum for the cubic pure lanthanide oxide (C-Ln_2O_3).

From a mechanistic point of view, the rate-determining step in the oxidative dehydrodimerization of methane, also known as the oxidative coupling of methane, OCM, is the rupture of the C–H bond to give CH_3 radicals which then recombine to yield ethane and later ethylene. Although this rupture is highly energetic (107 kcal/mol), it has been shown to occur at moderate temperatures on the surface of the catalyst.

The first hypothesis for this step was proposed by Lunsford *et al.* (3) and is based on a homolytic mechanism in which methane activation occurs via radical abstraction of a hydrogen atom from a methane molecule by ion-radical forms of oxygen present on the oxide catalyst surface,

$$\text{cat-}[O^-] + CH_4 \rightarrow \text{cat-OH} + CH_3^{\cdot}.$$

0021-9517/95 $12.00

This proposal was substantiated by the detection of oxygen ion radical O^- on the surface of Li/MgO catalysts (4) and it was assumed that the exchange of Mg ions by Li ions generates hole centers of the O^- type in the system.

More recently, Sokolovskii and co-workers proposed a mechanism involving a heterolytic fission of the methane C–H bond (2, 8–12). The activation would occur via an interaction with an acid–base pair from the surface, giving place to a proton detachment from the methane and formation of a methyl–metal compound in which the methyl is negatively charged.

$$Me^{2+}O^{2-} + CH_4 \rightarrow CH_3^-Me^{2+} + H^+O^{2-}$$

Further oxidation of these surface methyl anions would lead to methyl radicals, which then dimerize,

$$CH_3^-Me^{2+} \rightarrow CH_3^{\cdot} + Me^{2+} + e^-.$$

This mechanism has also been supported by the fact that all these catalysts are basic and there is a correlation between the basic centers and the catalytic activity; it is also supported by CH_4–CD_4 isotopic exchange experiments (13, 14).

Theoretical studies on methane activation on metal oxides are quite scarce, in contrast to the considerable effort devoted to the activation on pure transition metals. The homolytic rupture of the C–H bond induced by magnesium oxide has been the subject of few works (15–18), the most recent being those of Borve and Pettersson. These authors first carried out high-level calculations on gas-phase hydrogen abstraction (17) and later (18) took into account the effects due to the lattice following an elaborated model. The heterolytic possibility has been considered only by Kobayashi *et al.* (19, 20), who carried out HF-SCF and MP2 calculations on the chemisorption of CH_4 on the (100) MgO surface modeled by a Mg_4O_4 cluster.

In the present work, we report a detailed theoretical study of the methane activation on Al and La oxides by means of ab initio molecular orbital calculations. The main goal of this work is to obtain a deeper insight into methane chemisorption that could help us to understand better the strong difference in selectivity observed for catalysts depending on if they are based on either aluminum oxide or lanthanum oxide (γ-Al_2O_3 vs C–La_2O_3). Also, for catalysts where lanthanum ion is supposed to be part of the active site, we are interested in making clear the role played by the surrounding ionic arrangement, on which, as stated above, the selectivity is so dependent. The paper is arranged as follows: After a brief computational details section, results on the gas-phase methane activation by aluminum and lanthanum oxides will be reported. Here, fully optimized reaction pathways have been determined from ab initio Hartree–Fock calculations. In order to account for the ionic environment of the active sites, the effects due to the interaction between the cluster and the remaining part of the crystaL will be introduced in the last part of the work by using both point charges and ionic model potentials. The surfaces of the solids considered were γ-Al_2O_3, La_2O_3 supported on γ-Al_2O_3 for a loading of 10%, mixed $AlLaO_3$ oxide (perovskite), and C–La_2O_3.

COMPUTATIONAL DETAILS

Ab initio SCF calculations were undertaken using two strategies, depending on the type of approach. For the gas-phase models, the CH_4–$Al(OH)_3$ and CH_4–$La(OH)_3$ clusters were computed using the standard 6-31G basis set (21) for all atoms except lanthanun, for which the effective core potential approximation (22) to describe inner electrons was taken. For this atom, the valence basis set used (22) was ($10s5p3d$) contracted to [$4s2p2d$]. For these models, stationary points corresponding to reactants, transition state, and products were fully optimized at the RHF-SCF level. The stationary points on the potential energy hypersurface were characterized by computing the matrix of the second derivatives of the energy in a Cartesian representation. The energy profiles connecting the transition states to reactants and products were obtained using the intrinsic reaction coordinate method (23) as implemented in the HONDO program. In the surface-based models, embedded cluster calculations were performed in order to take into account environment lattice effects. Because of the highly ionic nature of aluminum and oxygen atoms in the solid, an adapted basis set was chosen. For Al, the basis set was ($8s5p1d$) contracted to [$5s3p1d$] derived from the Huzinaga original basis set (24), while for oxide ions, the ($11s7p$)/[$5s3p$] basis set optimized by Bagus *et al.* (25) was taken. For hydrogen and carbon atoms, the 6-31G basis set was enlarged with *p* and *d* functions (6-31G*dp* basis set). These calculations were performed in two stages. First, the geometry of hydrogen and methyl species on the surface were optimized, embedding the cluster in an array of charges. Then single-point calculations in which the first shells of ions are surrounded by model potentials were carried out. Details on how the surfaces were generated are given below. All the calculations were carried out using the HONDO-8.4 program (26) in a Convex C-240 minisupercomputer.

RESULTS AND DISCUSSION

Gas-Phase Approach

In order to have a first preview of the OCM catalytic process we have simulated the Al and La oxides by the

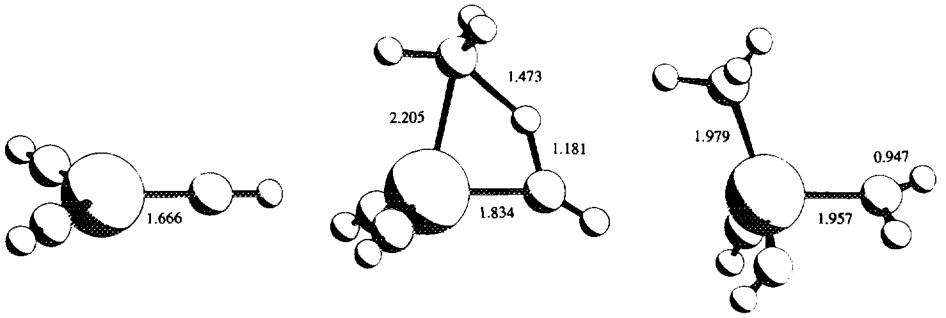

FIG. 1. Molecular structures for CH_4–$Al(OH)_3$ system optimized from RHF-SCF calculations. Left, $Al(OH)_3$; middle, transition state; right, methyl-aluminum carbanion (bond lengths are in Å).

neutral molecules $Al(OH)_3$ and $La(OH)_3$. Although these models can be considered too simple, they allow the use of well-known and efficient computational techniques for the search of stationary points based on analytical gradients. In Figs. 1 and 2, fully optimized structures for the systems CH_4–$Al(OH)_3$ and CH_4–$La(OH)_3$ are reported. As can be seen, both $Al(OH)_3$ and $La(OH)_3$ are plane, the interatomic metal–oxygen bond distance being 1.666 and 2.217 Å, respectively. When methane approaches on the right side, i.e., with a C–H bond almost parallel to a Me–O bond, there is an interaction between the basic center of the oxide and the methane hydrogen, giving rise to an increase in electron density on the methane carbon atom which, concomitantly, interacts with the Lewis acid center of the oxide. This double interaction leads to a four-center transition state in which the C–H bond is almost broken, as shown by the increment of this interatomic distance, while there is significant binding between the carbon and metal and, mainly, between the oxygen and hydrogen. Further evolution of these structures leads to products in which the methane activation has been achieved with formation of methyl–metal compounds. Mulliken population analysis of the products clearly shows the charge separation taking place in the reaction. Thus, the net charges of CH_3 groups are −0.47 and −0.58 for Al and La compounds, respectively, while for hydrogen the positive charge is almost the same in both products, 0.49.

Energy profiles for the methane activation by $Me(OH)_3$ are reported in Fig. 3. As can be seen, activation on lanthanum shows a late transition state with an activation barrier of 42.2 kcal/mol. Analysis of selected bond orders (27) reported in Table 1 agrees with the late character of the transition structure. The transition state for activation on aluminum appears somewhat earlier, and the energy barrier is of 46.3 kcal/mol. These activation barriers appear to be reasonable for a process involving the rupture of a highly energetic bond and can be viewed as upper bounds since neither polarization functions nor electron correlation effects are considered (28). However, they are in agreement with the value of 45 kcal/mol determined by Mirodatos and co-workers (14) from an experimental study on the exchange reaction

$$CH_4 + CD_4 \rightarrow CH_3D + CHD_3$$

catalyzed by magnesium oxide (pure or Li-doped), and for which a heterolytic mechanism was suggested.

While methane activation barriers on aluminum or lanthanum are close to each other, reaction energies appear to be quite different. Although both processes are endothermic, the methyl–lanthanum compound is computed to be considerably more energetic than the methyl-aluminum one, the reaction energies being 34.8 and 9.6 kcal/mol, respectively. Notice, on the other hand, that according to

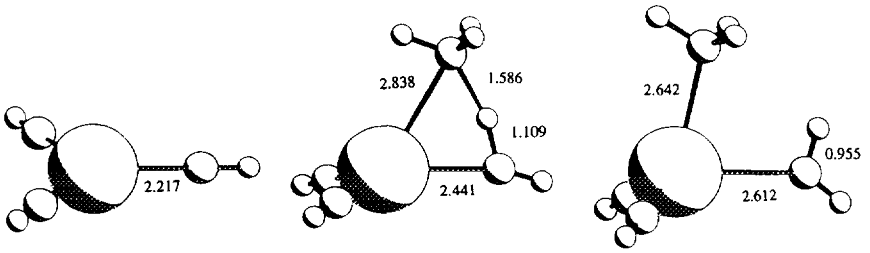

FIG. 2. Molecular structures for CH_4–$La(OH)_3$ system optimized from RHF-SCF calculations. Left, $La(OH)_3$; middle, transition state; right, methyl-lanthanum carbanion (bond lengths are in Å).

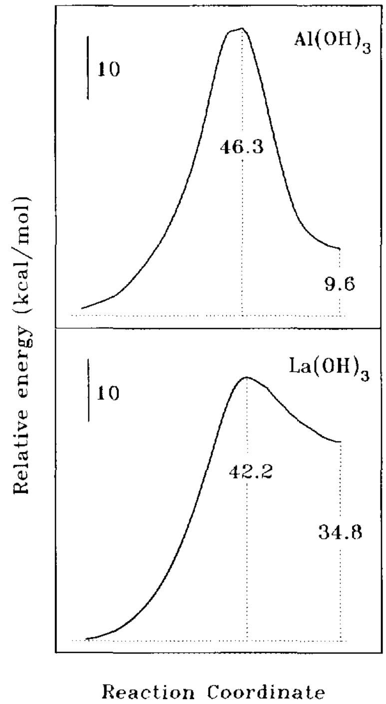

FIG. 3. Energy profiles for the activation of CH_4 by Me(OH)$_3$. Top, Me = Al; bottom, Me = La.

Hammond's principle, the endothermicity of these processes agrees with the fact that transition-state structures are closer to products.

The difference in the relative stabilities of the carbon–metal intermediates is in agreement with the stronger Lewis acidity of Al and suggests an explanation for the different selectivities found for these catalysts. Effectively, it is reasonable to assume that a lower stability of the methyl–metal intermediate will facilitate the formation of methyl radicals, the species whose dimerization gives rise to C2 products. Alternatively, more stabilized methyl–metal intermediates would feature further surface oxidation to give carbon oxides. This interpretation is in agreement with the trends observed in the selectivity for the lanthanide oxides series, in which the selectivity decreases on going from La_2O_3 to Lu_2O_3 (for a given structure), while the Lewis acidity rises on going from La to Lu (7, 29).

TABLE 1

Relative Energies and Selected Bond Orders for the Activation of CH_4 by Me(OH)$_3$ from RHF-SCF Calculations

	Reactants	T.s.	Product
Me = Al			
ΔE (kcal/mol)	0.0	46.3	9.6
B.O. (Al–O)	0.533	0.325	0.179
B.O. (C–H)	0.961	0.377	0.0
B.O. (Al–C)	0.0	0.339	0.755
B.O. (O–H)	0.0	0.302	0.735
Me = La			
ΔE (kcal/mol)	0.0	42.2	34.8
B.O. (La–O)	0.594	0.255	0.140
B.O. (C–H)	0.961	0.333	0.0
B.O. (La–C)	0.0	0.300	0.643
B.O. (O–H)	0.0	0.374	0.725

Note. Reactants stands for Me(OH)$_3$ and CH_4; T.s. stands for transition state; Product stands for the methyl–metal compound.

Surface Model Based Approaches

The simplest method to introduce the environment effects in a calculation is to embed the cluster in a set of point charges at the crystal positions. Usually, these Madelung-type potentials are calculated following an Ewald-based scheme (30), and then, a further fitting gives place to a finite set of charges simulating the potential created by the infinite solid. This method has been widely used and generalized for the most common structures (31). However, except for the $AlLaO_3$ and C–La_2O_3 solids, which have a clear regular structure, the method is not useful for γ-Al_2O_3 and derivatives in which a metal oxide is supported on it. Effectively, for γ-Al_2O_3 a spinel-like structure has been proposed (32) in which octahedral and tetrahedral aluminum ions are randomly distributed in such a way that 10% of tetrahedral sites and 46.7% of octahedral sites are occupied. This structure was idealized by Lippens *et al.* (33), who proposed a model in which the tetrahedral/octahedral ratio was preserved but, unfortunately, the stoichiometry was not correct.

Since one of the main concerns of our work was the suitability of model surfaces for catalysts, we have recently reported (34) on a molecular dynamics (MD) simulation of γ-Al_2O_3 which provided a model, taking into account the correct stoichiometry. From this structure, models for the different planes of γ-Al_2O_3 were also proposed (35). Also, MD simulations of the La_2O_3/γ-Al_2O_3 system at various loadings were carried out (36). These simulations were also the starting point for modeling the surfaces in the present work. Thus, for γ-Al_2O_3, the configuration arising from MD simulations of a cluster having the formula $Al_{576}O_{864}$, arranged in a cubic box, was cut by the (110) plane (the most likely exposed). Adopting this hemicube as the catalyst model, a cluster formed by one aluminum and three oxygens was selected at the center of the surface and treated explicitly while the rest of the ions were introduced into the calculations as point charges. Notice that these charges are not necessarily −2 and +3 but those used in the MD simulations (which ensures a proper description of periodicity conditions) and, therefore, small arrangements were needed in order to preserve the whole uncharged structure.

Starting from the MD simulations of the 10% La_2O_3/γ-Al_2O_3 mixture and following the previous procedure, a model structure for this catalyst was obtained. Finally, for evident reasons of homogeneity and for the sake of comparison, a similar scheme was used for $AlLaO_3$ and C–La_2O_3, although, because of their regularity, it was not strictly necessary. The surfaces were also those corresponding to the (110) plane except for the perovskite, for which the equivalent plane is (100).

Once the catalyst models were established, a hydrogen ion and a CH_3 group were placed on the surface and optimized, taking as starting point the geometries obtained for the methane activation on $Al(OH)_3$ and $La(OH)_3$ in the gas-phase approach. In these optimizations, the surfaces were kept frozen. The reaction energies were then calculated as the difference between the final structures and the energy of the catalyst plus that of free methane (Table 1). Bearing in mind the qualitative nature of these values, the following trends can be observed. First, when the activation occurs on aluminum oxide, the effect of the lattice is to stabilize the methyl–aluminum intermediate, the process now being clearly exothermic. The same effect is found when methane activation occurs via formation of a methyl–lanthanum compound. This general stabilization of the products can be understood by taking into account that the heterolytic rupture of C–H bonds produces a charge separation, which is stabilized by the electrostatic potential created by the point charges. Second, the energy shifts induced on the lanthanum oxide based catalysts strongly depend on the structure of the point charges arrangement. Thus, while for C–La_2O_3 and the 10% La_2O_3/γ-Al_2O_3 system there is a moderate lowering of energy, for the $AlLaO_3$ perovskite-type structure there is a large stabilization. This result could explain the differences observed in the selectivity of these catalysts. Effectively, assuming the inverse relation between the stability of the methyl–metal intermediate and the selectivity, as stated in the previous section, C–La_2O_3 and the 10% La_2O_3/γ-Al_2O_3 would be more selective than γ-Al_2O_3 and $AlLaO_3$, in agreement with the experiment.

In order to avoid the excessive polarization of the electronic cloud of the cluster due to the closest shells of ions, we also performed a set of single-point calculations at the optimized geometries in which a few layers of ions around the site were replaced by full ion model potentials instead of point charges. This procedure introduces short-range repulsions and has been shown to be a more realistic method of studying embedded cluster models (35, 36). In the present calculations we used spheric ab initio model potentials for oxide and aluminum ions, determined by following a technique (39) close to that of Huzinaga and co-workers (37, 38, 40) but in which model potentials were developed in a nonlocal representation (41). The number of ions replaced by model potentials was estimated after optimization; they were, in brief, all those falling inside an ellipsoid, focusing on the oxygen and Al (or La) on which the activation takes place (Fig. 4). As can be seen in Table 2 (m.p. entries), considerable effects on the reaction energies are observed. Except for γ-Al_2O_3, additional stabilization of the methyl–metal intermediates was introduced. However, although this approach changes the energetics, the qualitative picture depicted by using the point charges approach is preserved.

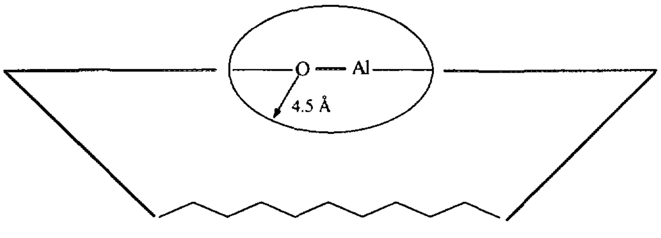

FIG. 4. Point charges–model potential representation of the surface. The ions falling inside the elipsoid are described by means of a model potential while the outer ions are replaced by point charges.

CONCLUDING REMARKS

In this work we have performed ab initio quantum mechanical calculations on the chemisorption of methane on Al and La oxides, the rate-determining step in the oxidative coupling of methane. For models CH_4–$Al(OH)_3$ and CH_4–$La(OH)_3$ fully optimized transition and product structures were determined. The transition states correspond to a four-center interaction between a methane C–H bond and a Al–O (or La–O) bond. The products are well described as methyl–metal compounds with the carbon negatively charged. For both processes activation barriers are large, about 40 kcal/mol, and are in agreement with those estimated for the hydrogen–deuterium exchange experiments of Mirodatos and co-workers (14) (45 kcal/mol), supporting the proposed heterolytic mechanism of this reaction.

TABLE 2

Reaction Energies (kcal/mol) Obtained by Using the Point Charge (P.C. Entries) and Model Potential-Point Charge (M.P. Entries) Models for the Activation of CH_4 on γ-Al_2O_3 and on La Sites of 10% La_2O_3/γ-Al_2O_3, $LaAlO_3$, and C–La_2O_3 Catalyst Surfaces

Catalyst	P.c.	M.p.
γ-Al_2O_3	−28	−22
10% La_2O_3/γ-Al_2O_3	5	1
$LaAlO_3$	−18	−21
C–La_2O_3	1	−4

Moreover, the barriers reported in this work have to be considered as upper bounds since as we have shown that a charge separation occurs during the C–H activation which will be favoured through electrostatic interaction with the lattice. On the other hand, Borve and Petterson (18), assuming a homolytic ruptue of the C–H bond of methane, reported from high-level calculations barriers of 7–10 Kcal/mol, in agreement with the principle that low energy barriers are expected for homolytic processes. Since most of the OCM reactions used to occur with considerably large barriers (42) our calculations strongly suggest that the heterolytic mechanism for such processes seems to be more likely.

In a summary, the reported study points out the fact that heterolytic splitting could occur under OCM conditions, but it would take place on basic sites (lattice oxides) without requiring the presence of adsorbed oxygen species, while the homolytic mechanism would occur on adsorbed oxygen as proposed by Lunsford (4).

The heterolytic mechanism also provides a guideline to rationalize the different selectivity towards C2 of these catalysts. The higher stability of the methyl–aluminum intermediate with respect to the methyl–lanthanum one would increase the possibility of further oxidation of such intermediates instead of a detachment of methyl radicals, the dimerization of which gives rise to C2 products. Assuming this inverse relation between the intermediate stability and the selectivity, we have found that C–La_2O_3 and low-loading La_2O_3 supported on γ-Al_2O_3 catalysts would be more selective than γ-Al_2O_3 and $AlLaO_3$, in agreement with experimental results.

ACKNOWLEDGMENTS

This work was financially supported by the Spanish D.G.I.C.Y.T., Project PB92-0662, and by the European Commission, Contract CI1-CT94-0064.

REFERENCES

1. Jones, C. A., Leonard, J. J., and Sofranko, J. A., *Energy Fuels* **1,** 12 (1987).
2. For a recent and exhaustive reviews, see Sokolovskii, V. D., and Mamedov, E. A., *Catal. Today* **14,** 331 (1992). [Part 4]
3. Ito, T., and Lunsford, J. H., *Nature (London)* **314,** 721 (1985).
4. Ito, T., Wang, J.-X. Lin, C.-H., and Lunsford, J. H., *J. Am. Chem. Soc.* **107,** 5062 (1985).
5. Wang, J.-X., and Lunsford, J. H., *J. Phys. Chem.* **90,** 5883 (1986).
6. Hutchings, G. J., Woodhouse, J. R., and Scurrell, M. S., *J. Chem. Soc. Faraday Trans.* **85,** 2507 (1989).
7. Capitán, M. J., Ph.D. thesis, University of Seville, 1993.
8. Sokolovskii, V. D., Aliev, G. M., Buyevskaya, O. V., and Davydov, A. A., *Catal. Today* **4,** 293 (1989).
9. Suleimanov, A. I., Ismailov, E. G., Aliev, S. M., and Sokolovskii, V. D., *React. Kinet. Catal. Lett.* **34,** 51 (1987).
10. Buyevskaya, O. V., Suleimanov, A. I., Aliev, S. M., and Sokolovskii, V. D., *React. Kinet. Catal. Lett.* **33,** 223 (1987).
11. Sokolovskii, V. D., *React. Kinet. Catal. Lett.* **35,** 337 (1987).
12. Davydov, A. A., Budevna, A. A., Aliev, S. M., and Sokolovskii, V. D., *React. Kinet. Catal. Lett.* **36,** 491 (1988).
13. Utiyama, M., Hattori, H., and Tanabe, K., *J. Catal.* **53,** 237 (1978).
14. Mirodatos, C., Holmen, A., Mariscal, R., and Martin, G. A., *Catal. Today* **6,** 601 (1990).
15. Mehandru, S. P., Anderson, A. B., and Brazdil, J. F., *J. Am. Chem. Soc.* **110,** 1715 (1988).
16. Zicovich-Wilson, C. M., Gonzalez-Luque, R., and Viruela-Martin, P. M., *J. Mol. Struct. (THEOCHEM)* **208,** 153 (1990).
17. Borve, K. J., and Pettersson, L. G. M., *J. Phys. Chem.* **95,** 3214 (1991).
18. Borve, K. J., and Pettersson, L. G. M. *J. Phys. Chem.* **95,** 7401 (1991).
19. Kobayashi, H. *Catal. Today* **10,** 167 (1991).
20. Ito, T., Tashiro, T., Kawasaki, M., Watanabe, T., Toi, K., and Kobayashi, H., *J. Phys. Chem.* **95,** 4476 (1991).
21. Hehre, W. J., Ditchfield, R., and Pople, J. A., *J. Chem. Phys.* **56,** 2257 (1972); Francl, M. M., Pietro, W. J., Hehre, W. J., Binkley, J. S., Gordon, M. S., DeFrees, D. J., and Pople, J. A., *J. Chem. Phys.* **77,** 3654 (1982).
22. Hay, P. I., and Wadt, W. R., *J. Chem. Phys.* **85,** 299 (1982).
23. Ishida, K., Morokuma, K., and Komornicki, A., *J. Chem. Phys.* **75,** 2800 (1981).
24. Huzinaga, S., Ed., "Gaussian Basis Sets for Molecular Calculations," Physical Science Data 16, Elsevier, Amsterdam, 1984.
25. Pachioni, G., Cogliandro, G., and Bagus, P. S., *Int. J. Quantum Chem.* **42,** 1115 (1992).
26. Dupuis, M., Chin, S., and Márquez, A., *in* "Chemstation and HONDO," *in* "Relativistic and Electron Correlation Effects in Molecules and Clusters" (G. Malli, Ed.), NATO ASI Series. Plenum, New York, 1992.
27. Villar, H. O., and Dupuis, M., *Chem. Phys. Lett.* **142,** 59 (1987), and references therein.
28. Hehre, W. J., Radom, L., Schleyer, P. v. R., and Pople, J. A., "Ab Initio Molecular Orbital Theory." Wiley, New York, 1986.
29. Centeno, M. A., Capitán, M. J., Bosch, P., Malet, P., Carrizosa, I., and Odriozola, J. A., *J. Catal.* **148,** 399 (1994).
30. Ewald, P. P., *Ann. Physik* **64,** 253 (1921).
31. Sousa, C., Casanovas, J., Rubio, J., and Illas, F., *J. Comput. Chem.* **14,** 680 (1993).
32. Verwey, E. J. W., *Z. Krist.* **91,** 317 (1935).
33. Lippens, B. C., *in* "Physical and Chemical Aspects of Adsorbents and Catalysts" (B. G. Linsen, Ed.), p. 171. Academic Press, New York, 1970.
34. Alvarez, L. J., Fernández Sanz, J., Capitán, M. J., and Odriozola, J. A., *Chem. Phys. Lett.* **192,** 463 (1992).
35. Alvarez, L. J., Fernández Sanz, J., Capitán, M. J., and Odriozola, J. A., *J. Chem. Soc. Faraday Trans.* **89,** 3623 (1993).
36. Alvarez, L. J., Fernández Sanz, J., Capitán, M. J., and Odriozola, J. A., *J. Mol. Struct. (THEOCHEM)* **287,** 161 (1993); Alvarez, L. J., Fernández Sanz, J., Capitán, M. J., and Odriozola, J. A., *Catal. Lett.* **21,** 89 (1993).
37. Barandiarán, Z., and Seijo, L., *J. Chem. Phys.* **89,** 5739 (1988).
38. Luaña, V., and Pueyo, L., *Phys. Rev. B* **41,** 3800 (1990).
39. Mejías, J. A., and Fernández Sanz, J., *J. Chem. Phys.* **99,** 1255 (1993).
40. Huzinaga, S., Seijo, L., Barandiarán, Z., and Klobukowski, M., *J. Chem. Phys.* **86,** 2132 (1987).
41. Mejías, J. A., and Fernández Sanz, J., *J. Chem. Phys.* **102,** 327 (1995).
42. See Ref. (2), p. 434.